Investigation of LiDAR Sensing Technology to Improve Freeway Traffic Monitoring

September 2022

A Research Report from the Pacific Southwest Region University Transportation Center

Stephen G. Ritchie, University of California, Irvine

Andre Tok, University of California, Irvine

Yiqiao Li, University of California, Irvine

Koti R. Allu, University of California, Irvine

TECHNICAL REPORT DOCUMENTATION PAGE

1. Report No. PSR-21-34	**2. Government Accession No.** N/A	**3. Recipient's Catalog No.** N/A
4. Title and Subtitle Investigation of LiDAR Sensing Technology to Improve Freeway Traffic Monitoring		**5. Report Date** 1/30/23 **6. Performing Organization Code** N/A
7. Author(s) Stephen G. Ritchie, Andre Tok, Yiqiao Li, Koti R. Allu & Jared Sun		**8. Performing Organization Report No.** TBD
9. Performing Organization Name and Address METRANS Transportation Center University of Southern California University Park Campus, RGL 216 Los Angeles, CA 90089-0626		**10. Work Unit No.** N/A **11. Contract or Grant No.** USDOT Grant 69A3551747109 CALTRANS TO 049
12. Sponsoring Agency Name and Address U.S. Department of Transportation Office of the Assistant Secretary for Research and Technology 1200 New Jersey Avenue, SE, Washington, DC 20590		**13. Type of Report and Period Covered** Final report (Oct 2021 – Sep 2022) **14. Sponsoring Agency Code** USDOT OST-R
15. Supplementary Notes		

16. Abstract

LiDAR is an emerging technology that can provide detailed point-cloud measurements for accurate detection and characterization of objects. The cost of this technology has seen significant reduction in recent years with the scaling of production to meet the demands of wide-ranging applications such as autonomous vehicles, infrastructure inventory and topographic mapping, to name a few. Within the field of infrastructure-based traffic monitoring, recent studies have investigated the use of this sensor for advanced truck classification applications in side-fire orientation, as well as for motorized vehicle, bicycle and pedestrian detection at traffic intersections. This study explored the potential of LiDAR in traffic monitoring applications. These include the investigation in the feasibility of edge-side data processing of real-time LiDAR data, real-time detection of vehicle objects using a state-of-the-art object detection algorithm and the use of LiDAR to estimate microscopic vehicle trajectories within its field of view.

17. Key Words LiDAR, ROS, Object Detection, Microscopic Trajectory		**18. Distribution Statement** No restrictions.	
19. Security Classif. (of this report) Unclassified	**20. Security Classif. (of this page)** Unclassified	**21. No. of Pages** 49	**22. Price** N/A

Form DOT F 1700.7 (8-72) Reproduction of completed page authorized

Contents

About the Pacific Southwest Region University Transportation Center

The Pacific Southwest Region University Transportation Center (UTC) is the Region 9 University Transportation Center funded under the US Department of Transportation's University Transportation Centers Program. Established in 2016, the Pacific Southwest Region UTC (PSR) is led by the University of Southern California and includes seven partners: Long Beach State University; University of California, Davis; University of California, Irvine; University of California, Los Angeles; University of Hawaii; Northern Arizona University; Pima Community College.

The Pacific Southwest Region UTC conducts an integrated, multidisciplinary program of research, education and technology transfer aimed at *improving the mobility of people and goods throughout the region.* Our program is organized around four themes: 1) technology to address transportation problems and improve mobility; 2) improving mobility for vulnerable populations; 3) Improving resilience and protecting the environment; and 4) managing mobility in high growth areas.

U.S. Department of Transportation (USDOT) Disclaimer

California Department of Transportation (CALTRANS) Disclaimer

Disclosure

Principal Investigator, Co-Principal Investigators, others, conducted this research titled, "Investigation of LiDAR Sensing Technology to Improve Freeway Traffic Monitoring" at the

Institute of Transportation Studies, University of California, Irvine. The research took place from Oct 2021 to Sep 2022 and was funded by a grant from the Pacific Southwest Region University Transportation Center in the amount of $127,592. The research was conducted as part of the Pacific Southwest Region University Transportation Center research program.

Acknowledgements

The authors would like to extend their sincere appreciation to the staff from Caltrans Districts 7, 8 and 11 for providing access to traffic cabinets and their assistance with the installation of the LiDAR sensors and mountain hardware.

Abstract

LiDAR is an emerging technology that can provide detailed point-cloud measurements for accurate detection and characterization of objects. The cost of this technology has seen significant reduction in recent years with the scaling of production to meet the demands of wide-ranging applications such as autonomous vehicles, infrastructure inventory and topographic mapping, to name a few. Within the field of infrastructure-based traffic monitoring, recent studies have investigated the use of this sensor for advanced truck classification applications in side-fire orientation, as well as for motorized vehicle, bicycle and pedestrian detection at traffic intersections. This study explored the potential of LiDAR in traffic monitoring applications. These include the investigation in the feasibility of edge-side data processing of real-time LiDAR data, real-time detection of vehicle objects using a state-of-the-art object detection algorithm and the use of LiDAR to estimate microscopic vehicle trajectories within its field of view.

Investigation of LiDAR Sensing Technology to Improve Freeway Traffic Monitoring

Executive Summary

LiDAR is an emerging technology that can provide detailed point-cloud measurements for accurate detection and characterization of objects. The cost of this technology has seen significant reduction in recent years with the scaling of production to meet the demands of wide-ranging applications such as autonomous vehicles, infrastructure inventory and topographic mapping, to name a few. Within the field of infrastructure-based traffic monitoring, recent studies have investigated the use of this sensor for advanced truck classification applications in side-fire orientation (by the ITS-Irvine research team[1]), as well as for motorized vehicle, bicycle and pedestrian detection at traffic intersections. Because of the ability to obtain detailed three-dimensional reconstruction of vehicles from the preceding research by ITS-Irvine, traffic surveillance models developed for this sensor technology possess some inherent advantages over existing technologies such as inductive loops and microwave radar in traffic stream measurements, as well as vehicle count and classification accuracies for traffic monitoring and census applications. This potentially applies to both permanent freeway locations and temporary work zone locations. In particular, our research to date[2] suggests that LiDAR has the potential to be a cost-effective substitute for inductive loop sensors at permanent and temporary traffic surveillance and monitoring sites where overhead mounting infrastructure is available.

Four sites were selected for LiDAR point cloud data collection for this study as shown in Figure ES-1. These sites are part of the University of California, Irvine Institute of Transportation Studies (UCI-ITS) Freight Mobility Living Laboratory (FML2) deployment of advanced detector sites and were strategically located to monitor a diverse population of trucks and their activity. The I-15 Mountain Pass and I-10 Blythe study sites are located near the state borders with Nevada and Arizona, respectively, to capture interstate truck movements. The I-710 Willow study site is located near the Ports of Los Angeles and Long Beach, and is ideal for monitoring drayage truck activity. The SR-7 study site serves the Calexico truck border crossing, and is located just south of the intersection with the SR-98 highway. These four sites are also part of the UCI ITS network of Truck Activity Monitoring System (TAMS) sites throughout the State of California, which provides truck data in detailed body and axle classification data using existing inductive loops sensor infrastructure.

Installation of field sensors at each site was performed in coordination with Caltrans District field staff. The LiDAR sensors were installed on an existing gantry or poles that were secured to traffic cabinets with the assistance of Caltrans field staff for this study. Each study site is equipped with a combination of a LiDAR sensor, an Automatic License Plate Recognition (ALPR)

[1] Li Y., K.R. Allu, Z. Sun, A. Tok, S.G. Ritchie, 2021. An Ensemble Approach to Truck Body Type Classification using Deep Representation Learning on 3D Point Sets. Proceedings of the 100th Annual Meeting of the Transportation Research Board, Washington D.C.

Camera, advanced signature-capable inductive loop detectors, and a solid-state field processing unit.

Figure ES-1 Location of Study Sites

This study involved three main tasks (organized in Chapters 3 thru 5) in exploring the use of LiDAR sensors for obtaining traffic performance measures. The first task investigated the feasibility of edge-side point cloud data processing from real-time LiDAR data using a platform known as the Robotic Operating System (ROS). This involved exploring several essential steps needed to prepare an operational field system to perform LiDAR-based traffic data collection. The main components of this system are a sensor driver used to establish communication between the LiDAR sensor and field unit, a data parser to interpret the raw sensor data stream into the desired measurement data to provide near real-time LiDAR data processing at the edge-side.

The second task involved the evaluation of traditional image-based processing methods used to perform vehicle detection and the investigation of deep learning-based LiDAR object detection methods to address data processing challenges associated with the real-time detection of vehicle objects. The investigation involved the implementation of PointPillar (Figure ES-2) – a state-of-the-art pre-trained object detection algorithm originally developed for autonomous driving applications – for traffic monitoring applications.

Pacific Southwest Region UTC
University Transportation Center

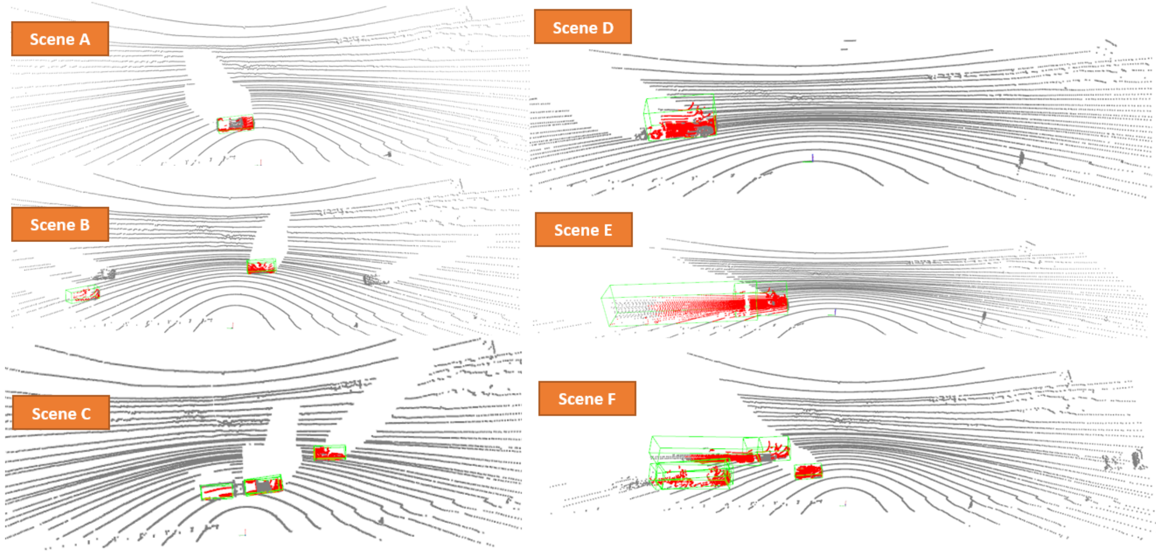

Figure ES-3 PointPillar Detection Results

The final task explored the use of LiDAR data to estimate the microscopic trajectories within its field of view (FOV). Microscopic trajectories can be used to study various traffic flow phenomena such as car-following behavior, lane changing behavior, capacity drop and traffic oscillation propagation. LiDAR technology has significant potential in these applications due to its ability to directly measure physical attributes of vehicle objects. However, a fixed reference point such as the centroid of a vehicle – which is essential for trajectory estimation across captured frames – cannot be reliably obtained if only an incomplete part of a vehicle is captured in each frame. This is especially prevalent near the FOV extremes, where vehicles are entering and exiting its view, or when vehicles are occluded by other vehicles in adjacent lanes. The first step in this task involved a comprehensive literature review of trajectory estimation techniques followed by the development of a methodological framework to process raw LiDAR data and combine the individual frames of LiDAR scans of a vehicle through a process known as registration. An investigation of available registration algorithms was performed to determine the optimal registration pipeline. Finally, the estimated microscopic trajectory (example shown in Figure ES-3) was obtained by performing sequential inverse rigid body transformations of the reconstructed vehicle body.

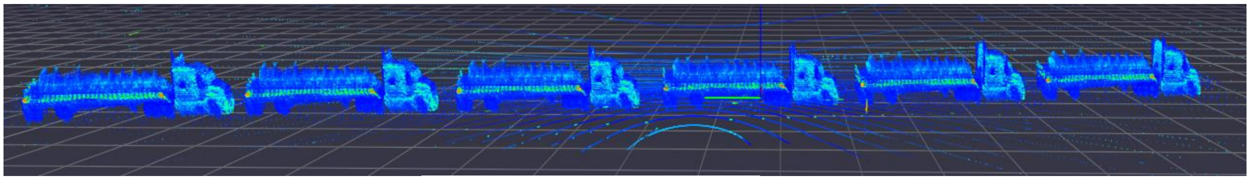

a. Side View

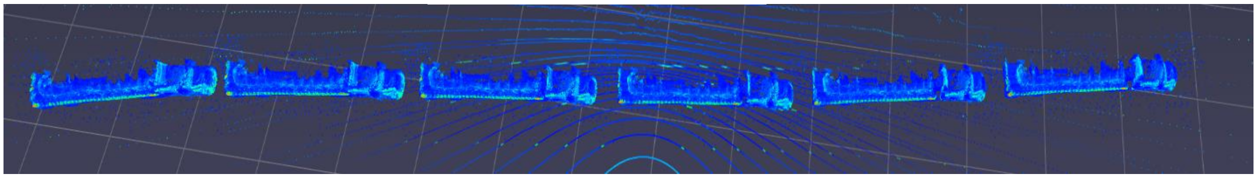

b. Top View

Figure ES-3 An Example of Microscopic Trajectory presented at 1 second aggregation from reconstructed LiDAR scans

Chapter 1 Introduction

LiDAR is an emerging technology that can provide detailed point-cloud measurements for accurate detection and characterization of objects. The cost of this technology has seen significant reduction in recent years with the scaling of production to meet the demands of wide-ranging applications such as autonomous vehicles, infrastructure inventory and topographic mapping, to name a few. Within the field of infrastructure-based traffic monitoring, recent studies have investigated the use of this sensor for advanced truck classification applications in side-fire orientation (by the ITS-Irvine research team[2]), as well as for motorized vehicle, bicycle and pedestrian detection at traffic intersections. Because of the ability to obtain detailed three-dimensional reconstruction of vehicles from the preceding research by ITS-Irvine (as shown in Figure 1-1), traffic surveillance models developed for this sensor technology have some inherent advantages over existing technologies such as inductive loops and microwave radar in traffic stream measurements, as well as vehicle count and classification accuracies for traffic monitoring and census applications. This potentially applies to both permanent freeway locations and temporary work zone locations. In particular, our research to date[2] suggests that LiDAR has the potential to be a cost-effective substitute for inductive loop sensors at permanent and temporary traffic surveillance and monitoring sites with available overhead mounting infrastructure.

This study sought to investigate the potential use of LiDAR technology in obtaining traffic performance measures. A recurring concern of LiDAR is in its significant computational requirements due to the large data throughput from the sensor. Hence, edge side computing was investigated to determine the feasibility for traffic operations applications. This investigation explored real-time data processing platforms such as the Robotic Operating System (ROS) and deep-learning-based object detection methods. An investigation was also made to develop a model to obtain microscopic trajectory estimation from individual raw LiDAR frames. Data was obtained from LiDAR sensors installed at several Freight Mobility Living Laboratory (FML2) testbed locations along existing freeway corridors in Southern California.

[2] Li Y., K.R. Allu, Z. Sun, A. Tok, S.G. Ritchie, 2021. An Ensemble Approach to Truck Body Type Classification using Deep Representation Learning on 3D Point Sets. Proceedings of the 100th Annual Meeting of the Transportation Research Board, Washington D.C.

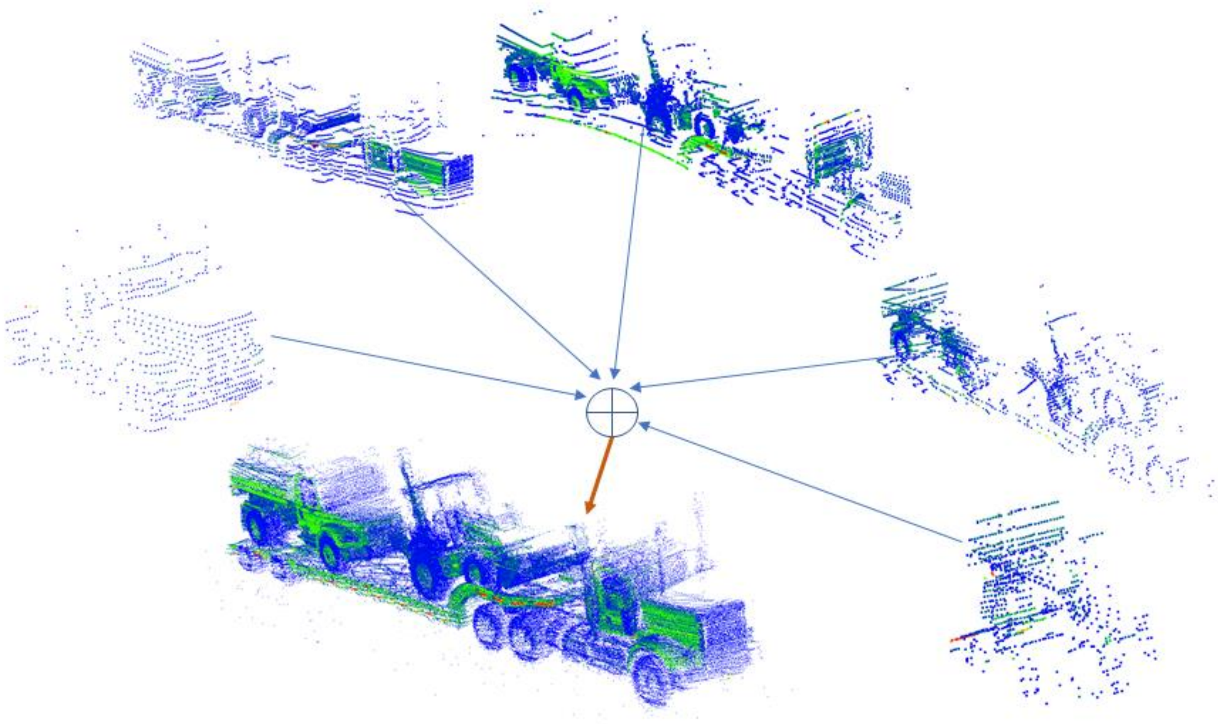

Figure 1-1 Detailed three-dimensional reconstruction of a truck from LiDAR point cloud data

Chapter 2 Field Equipment Setup and Data Collection

2.1 Overview

Four study sites were selected for LiDAR point cloud data collection. These sites were strategically located to monitor a diverse population of trucks and their activity, as shown in Figure 2-1. The I-15 Mountain Pass and I-10 Blythe study sites are located near the state borders with Nevada and Arizona, respectively, to capture interstate truck movements. The I-710 Willow study site is located near the Ports of Los Angeles and Long Beach, and is ideal for monitoring drayage truck activity. The SR-7 study site is located just south of the intersection with SR-98 highway, and serves the Calexico truck border crossing. The inductive loop sensors at all four sites are connected to advanced signature-capable detector cards as part of the UCI ITS network of Truck Activity Monitoring System (TAMS) sites, which provides truck data in detailed body and axle configurations using existing inductive loop sensors.

Figure 2-1 Location of Study Sites

Installation of field sensors at each site was performed in coordination with Caltrans District field staff. The LiDAR sensors were installed on an existing gantry or poles that were secured to traffic cabinets with the assistance of Caltrans field staff for this study. Each detection site is equipped with a combination of a LiDAR sensor, an Automatic License Plate Recognition (ALPR) Camera, advanced signature-capable inductive loop detectors, and a solid-state field processing unit. Figure 2-2 shows an example of advanced sensors installed at the I-10 Blythe study site.

Figure 2-2 Example of Sensor Installation at Blythe Study Site

2.2 Description of Study Sites and Equipment Setup

2.2.1 I-15 Mountain Pass Prepass WIM Site

The I-15 Mountain Pass site (shown in Figure 2-3) is located along the single-lane truck bypass between the state agricultural inspection facility and the commercial vehicle enforcement facility at an existing PrePass Weigh-In-Motion (WIM) site, which monitors all truck activity traveling southbound from Nevada entering into California. A VLP-16 LiDAR sensor was secured to the vertical mast of the existing PrePass gantry and powered from the traffic cabinet via a Power-Over-Ethernet (POE) connection. Additional hardware at this study site include WIM sensors, an inductive loop sensor connected to signature-capable inductive loop detector card and an Automatic License Plate Recognition (ALPR) Camera. The on-site field processing unit was located in the traffic cabinet and archived data from the traffic sensors.

Figure 2-3 I-15 Mountain Pass Study Site Setup

2.2.2 I-10 Blythe Traffic Census Site

The I-10 Blythe study location (shown in Figure 2-2) is an existing Caltrans Traffic Census site which monitors all mainline interstate traffic with two lanes in each direction. A VLP-32C LiDAR sensor was installed on a pole secured to the traffic cabinet next to the westbound lanes entering California.

This study site is also equipped with an ALPR unit as well as a video camera for the validation of vehicle records.

2.2.3 SR-7 Calexico Traffic Census Site

The SR-7 Calexico study location is an existing Caltrans Traffic Census site equipped with piezo and inductive loop sensors located about a quarter mile north of the United States – Mexico truck border crossing at Calexico. The SR-7 highway at this location comprises two mainline lanes in each direction (shown in Figure 2-4). The traffic cabinet location adjacent to the northbound lanes allows the LiDAR sensor to monitor truck movements from Mexico entering through the border crossing into California.

Pacific Southwest Region UTC
University Transportation Center

Figure 2-4 Equipment Setup at SR-7 Calexico

2.2.4 I-710 Willow Traffic Monitoring Site

The study site along the I-710 Interstate freeway (shown in Figure 2-5) was set up to monitor drayage truck activity from the Ports of Los Angeles and Long Beach. The I-710 freeway at this location comprises three mainline lanes in both the northbound and southbound directions.

Figure 2-5 Equipment Setup at I-710 Willow

2.3 Data Collection

LiDAR point cloud data was collected continuously over the time periods shown in Table 2-1 to test its ability for long-term traffic data collection.

Table 2-1 Data Collection period for Four Detection Sites

Detection Site	Data Collection Period
I-10 @ Blythe	May 5 2022 – Jul 2 2022
I-710 n/o Willow St	Mar 6 2022 – Jun 11 2022
I-15 @ Mountain Pass	Mar 1 2022 – Apr 20 2022
SR-7 s/o SR-98	Mar 1 2022 – Apr 16 2022

Chapter 3 Investigation of Edge-side LiDAR Data Processing using Robotic Operation System (ROS)

Several essential steps are needed to prepare a field computing unit equipped with LiDAR for traffic data collection. First, a sensor driver is used to establish communication between the LiDAR sensor and field unit. Second, a data parser is required to interpret the raw sensor data stream into the desired measurement data. Thus, an integrated platform is required to facilitate efficient LiDAR data collection and processing. In this chapter, we investigated the use of the open-source platform – Robotic Operation System (ROS)[3] – to provide near real-time LiDAR data processing at the edge-side. This chapter is organized as follows. First, a brief introduction to ROS is presented. Second, we describe our data collection setup and the collected datasets. Finally, we show a real-time data visualization result using ROS to present the feasibility of the use of ROS to process sensor data and deploy models.

3.1 Introduction to ROS

Robotic Operation System (ROS) is an open-source software development kit that comprises a set of libraries and tools that was initially designed for the use of robotics applications. ROS provides sensor drivers and an array of state-of-the-art data processing algorithms to facilitate tasks ranging from data streaming to modeling and implementation of robotic projects. This platform has also been adopted in the development of the autonomous driving platform.

ROS can be considered as a meta-operation system containing tool and libraries in addition to built-in Operation System functions, such as hardware abstractions, package management and a developer toolchain[4]. ROS comprises three levels of concepts: the Filesystem level, the Computation Graph level, and the Community level.

Resources are organized on the hard disk ROS filesystem level. The building blocks of the filesystem are described in Table 3-1.

Table 3-1 Concepts of Filesystem Level Components

	Descriptions
Packages	- Basic unit in ROS - Contains runtime process (nodes), libraries, configuration files, etc.
Package Manifest	- A file inside a package - Contains information about the package such as author, dependencies, etc.
Meta Packages	- A group of packages used for a special purpose.
Meta Packages Manifest	- Like the package manifest - Include packages inside as runtime dependencies and declare a runtime tag. - A client calls the service by sending the request message and awaiting a reply.
Messages	- A type of Information that is sent among ROS processes - A custom message can be defined.

[3] ROS: https://www.ros.org/
[4] Understanding the ROS filesystem level: https://subscription.packtpub.com/book/hardware-&-creative/9781788478953/1/ch01lvl1sec13/understanding-the-ros-filesystem-level

Services	- A kind of request/reply to interaction between processes.

The Computation Graph level is the most essential concept needed to understand the overall system. It is a peer-to-peer network of ROS processes that process data together. As shown in Figure 3-1, the basic ROS Computational Graph is comprised of Nodes, Masters, Parameter Servers, Messages, Services, Topics, and Bags. A summary of ROS Computation Graph components is presented in Table 3-2.

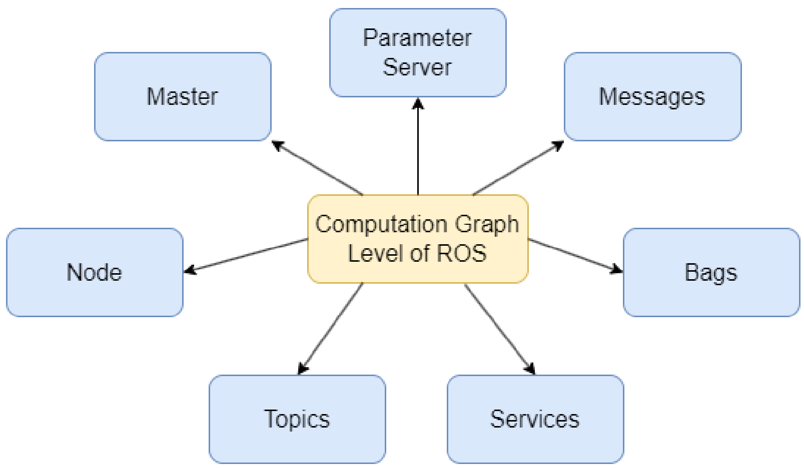

Figure 3-1 Computation Graph Level of ROS

Table 3-2 Concepts of ROS Computation Graph Components (*1*)

	Descriptions
Nodes	- Nodes are processes that perform computation - Each node performs a specific task
Master	- The ROS Master is a server that provides name registration and lookup to the rest of the computation graph - Nodes rely on the Master to find each other, exchange messages or invoke services
Parameter Server	- Parameter server allows data to be stored by key in a central location
Messages	- Nodes communicate with each other via messages - A message is a data structure comprising typed fields
Topics	- Messages travel through a transport system via publish/subscribe semantics. A node sends out messages via publishing it to a given topic. - Topics are names used to identify the content of messages
Services	- Request/reply in the publish/subscribe communication paradigm is accomplished by a Service, which is defined by a pair of messages: one for the request and one for the reply. - A client calls the service by sending the request message and awaiting a reply.
Bag	- ROS bags are a format for saving and playing back ROS message data.

The Community level concepts are used for different communities to exchange knowledge. It contains Distributions (similar to Linux distributions), Code Repositories, ROS Wiki, etc.

3.2 Real-Time Data Streaming and Visualization with ROS

The first task was to demonstrate real-time data streaming and visualization using ROS. Figure 3-2 demonstrates how the raw LiDAR packets from VLP-32c was processed and displayed through ROS.

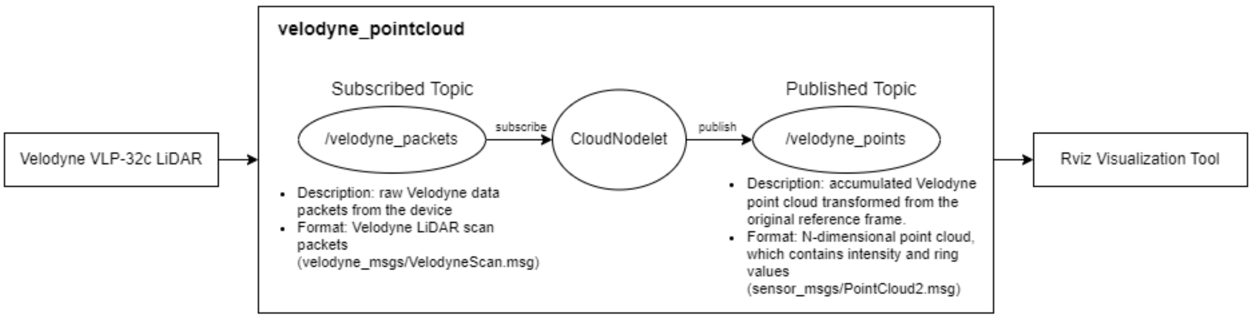

Figure 3-2 ROS LiDAR Data Visualization

Here, a point cloud conversion package designed for Velodyne Sensors was used to convert raw LiDAR packets received from VLP-32c to points stored in a format of Cartesian coordinate with additional information including “intensity” and “ring” values. Within this package, the “CloudNodelet” nodelet subscribed “/velodyne_packets” topic which contains the raw Velodyne data packets and published them to “/velodyne_points” topic, which holds the accumulated Velodyne point cloud transformed from the original reference frame. After that, we started the ROS graphical interface Rviz and subscribed to “velodyne_points” topic to display the 3D point cloud in the visualizer. The entire process is performed within the edge computing unit. The real-time point cloud visualization is displayed in Figure 3-3.

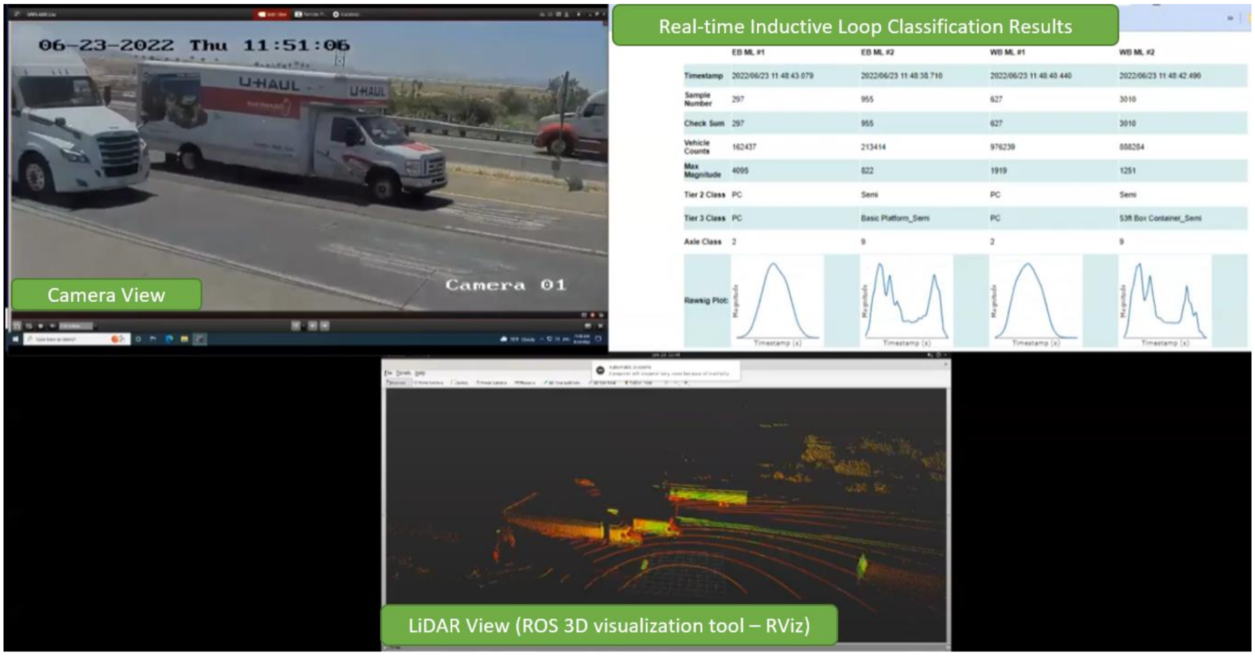

Figure 3-3 Real-time Point Cloud Visualization

The top left corner in Figure 3-3 shows the camera view of the I-10 Blythe detection site, and the top right corner presents the live classification results from the inductive loop detector. Correspondingly, the RViz interface visualizes the real-time LiDAR data stream through the ROS platform.

Chapter 4 Investigation of Deep Learning-based LiDAR Object Detection Methods for Roadside Applications

4.1 Introduction to Vehicle Detection

Vehicle object detection is an essential task within LiDAR-based traffic data acquisition frameworks. LiDAR-based object detection methods that have been found in literature can be summarized into two categories: traditional image processing methods and learning-based methods. This chapter first presents the literature on both methods and then discusses the object detection issues observed using the traditional methods from the collected dataset. Next, the chapter explores the existing learning-based object detection models which have been previously used for autonomous vehicle perception and investigates the use of pre-trained models for roadside applications. Finally, this chapter discusses the potential improvement methods for roadside LiDAR-based truck detection models and proposes future research directions.

4.1.1 Traditional Image Processing Methods for Vehicle Detection

The traditional method to extract vehicle objects from the background environment is to first filter out background points according to their physical characteristics and then group the foreground vehicle objects using clustering methods. This type of method assumes that the background is static and then pre-selects multiple frames without any foreground objects as background frames (*2*–*4*). Subsequently, the target frames which contain vehicle objects will be compared with the background frame. The target point is identified as a point belonging to an object if the distance between the target point and background points is larger than a certain threshold. Finally, a density-based clustering method – Density-based Spatial Clustering of Applications with Noise (DBSCAN) – is adopted to group foreground points as vehicle objects and distinguish dissimilar objects. Similarly, we also considered using the maximum laser range distance values to eliminate static background points and subsequently used the Euclidean Cluster Extraction Algorithm to detect moving vehicles (*5*). In addition, to compare the raw point, Wu et al. developed a background subtraction method by segmenting the 3D space into cubes and filtering out the background cubes based on the cumulative cube density across multiple frames and then using the DBSCAN method to detect vehicle objects (*6*, *7*). This method reduced the computation time effectively and is able to filter out some moving background objects. Later, researchers also made efforts on enhancing the background subtraction processing by introducing and extracting additional sensor information such as Azimuth-Height (*8*) and intensity (*9*) values to support a better object detection result.

The aforementioned methods were performed on limited datasets collected over a short time period within a day. However, we observed significant background shift issues in the proximity of sunrise and sunset. We suspect that the shifts may be caused by the temperature changes that may alter the alignment of the LiDAR sensors through distortion of the mounting pole. This results in a background that may deviate from its static reference points. Since the previous methods rely on using multiple background frames as inputs, that method could fail due to the temperature-affected transient changes of the background frames. In addition, the traditional unsupervised object detection methods utilized the spatial relationships between points to group points as vehicle objects. However, the shape of the vehicle objects was not well-considered. Thus, the detection results could be affected by the density distribution of the vehicle objects, especially for tractor-trailer trucks, since those algorithms recognized the object clusters based on the distance between each point within the object.

4.1.2 Deep Learning-based Methods

The development of autonomous driving in recent years has facilitated the rapid growth of deep learning-based 3D object detection models, with significant improvements in robustness, reliability, and computationally efficiency. Like the task of 2D image object detection models (e.g. R-FCN (*10*), R-CNN (*11*), Faster R-CNN (*12*), SSD (*13*), YOLO (*14*)), 3D detection models can be categized into two major types: One-stage and Two-stage models. One-stage detectors perform object classification and bounding-box regression directly without generating region proposals. On the other hand, two-stage models comprise two parts: a proposal generator followed by a detection generator. This type of detector will first generate region proposals and subsequently perform object classification for each proposed region. Two-stage models generally have better accuracy compared to one-stage models. However, they are more computationally intensive than one-stage models. Both types of models have been used in perception tasks of autonomous driving. Li et al. made the first attempt to apply a one-stage fully convolutional network detection method on the 2D point map which is projected and discretized from a 3D point cloud obtained from a LiDAR sensor (*15*). However, the 3D information from the sensor was not fully utilized. To further enhance the detection accuracy, researchers developed a 3D CNN model to extract features from the voxel representation of the point cloud (*16*). However, the efficiency of the voxel representation is relatively low compared to 2D models. To balance the detection accuracy and the computation efficiency, Yang et al. designed a single-stage PIXOR (Oriented 3D object detection from PIXel-wise neural network predictions) detector (*17*). They represent the 3D scene from the bird's eye view (BEV) to reduce computation and use the height as channels along the third dimension to preserve the 3D information. Furthermore, Lang et al. designed a novel fast encoder for the task of 3D object detection named PointPillar (*18*). PointPillar utilized the PointNets (*19*) to learn the representation of point clouds based on their vertical columns which are called pillars in their study. Subsequently, the extracted features will be scattered and projected back to a 2D pseudo-image as an input for a 2D CNN backbone. Finally, the SSD detector has been adopted as the detection head and produces prediction results. Several two-stage models such as DepthCN (*20*), MV3D (*21*), and PointRCNN (*22*) have been designed for autonomous vehicle perception tasks. However, their computation efficiency is presented as their main concern. In addition to the object detection model development, several autonomous vehicle datasets deserve mention, such as Waymo (*23*), Lyft (*24*), KITTI (*25*), and nuScenes (*26*) dataset. These datasets provide a large amount of labelled 3D objects collected through autonomous vehicles from the on-road scene. The LiDAR sensors are placed horizontally on the top of the vehicle to perceive the ambient environment. These datasets have been considered as benchmark datasets that are used to develop and compare 3D object detection models across academia and industry.

In this study, we explored the use of a pre-trained state-of-the-art object detection – PointPillar - for the task of roadside truck monitoring and performed qualitative analysis on our roadside LiDAR dataset.

4.2 Implementation of Pre-trained Object Detection Algorithms

4.2.1 Ground Plane Regression and Sensor Orientation Adjustment

To reduce the occurrence of occlusion issues and capture the inner-lane traffic, the LiDAR was mounted around 2.5 meters above the ground. However, lasers are unevenly distributed on the LiDAR rotating platform. The lasers are densely distributed in the area with smaller elevation angles (Figure 4-1 and Figure 4-2) and sparsely distributed with larger evaluations. When the sensor was placed horizontally and parallel to the ground plane, the point cloud obtained from the sensor will be too sparse to extract useful traffic information. Therefore, we slightly tilted the LiDAR to allow the center line of the sensor to point toward the region of interest (Figure 4-3).

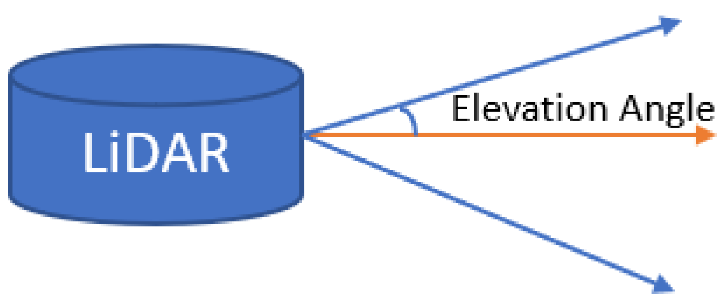

Figure 4-1 Illustration of Elevation Angles

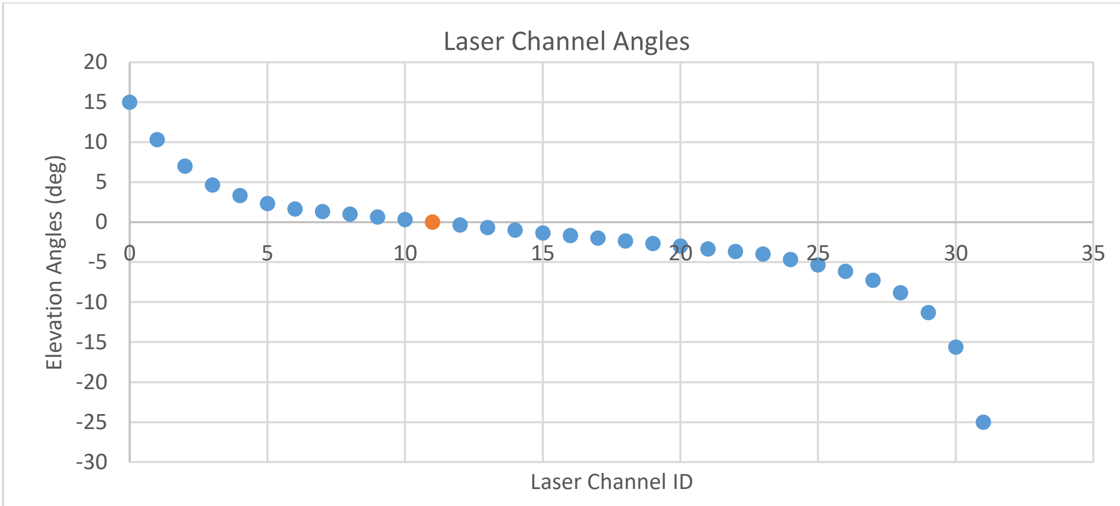

Figure 4-2 Laser Channel Angles Distribution

However, PointPillar converts raw point cloud to a stacked pillar tensor and pillar index tensor, which assumes the center line of the LiDAR is parallel to the ground plane. Thus, for our roadside vehicle detection task, we need to transform the sensor coordinate to align with the ground plane. First, the ground plane within the region of interest was estimated through the Random sample consensus (RANSAC) algorithm (*27*). The plane equation in the cartesian coordinate is shown in Equation 1.

$$ax + by + cz + d = 0 \tag{1}$$

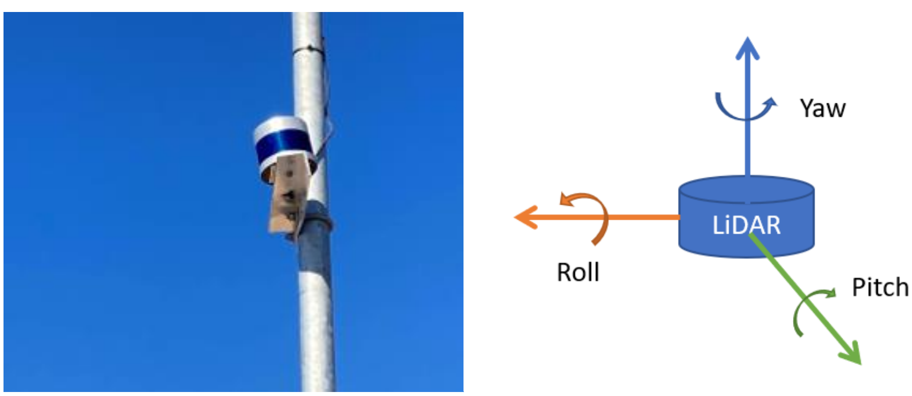

Figure 4-3 LiDAR Sensor Orientation

Subsequently, the yaw, roll, and pitch values of the LiDAR sensor are calculated through the transformation matrix between the ground plane equation and the original LiDAR sensor coordinate. Finally, the sensor orientation is adjusted according to the yaw, roll, and pitch values. The sensor adjustment result is present in Figure 4-4.

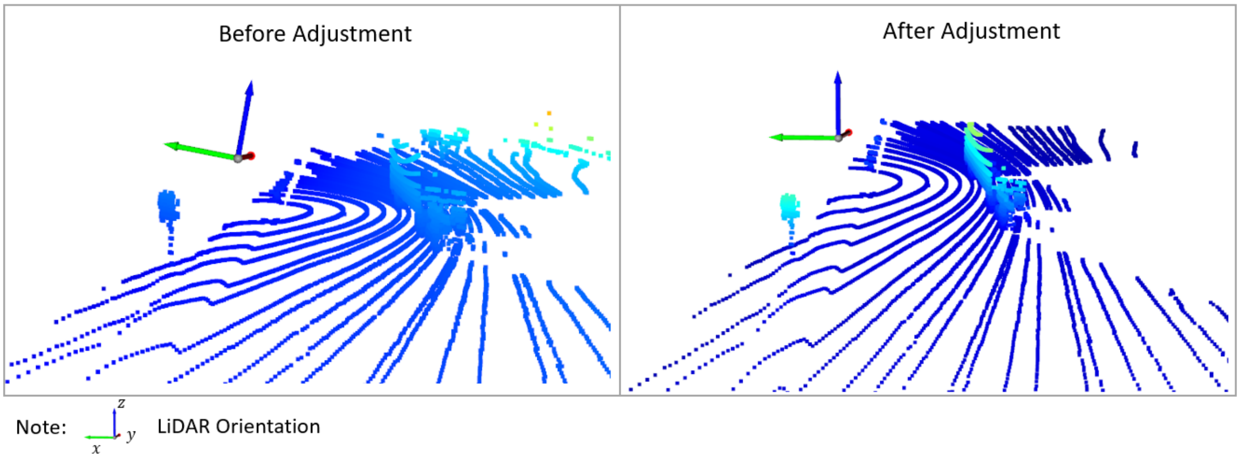

Figure 4-4 Sensor Orientation Adjustment

4.2.2 Qualitative Analysis of the Deep Learning Object Detection Model

In this study, the PointPillar model that had been pre-trained on the nuScenes dataset was tested for roadside passenger vehicle and truck detection. As shown in Figure 4-5 Scene A, the detection model was capable of successfully capturing the passenger vehicles that are located close to the sensor. However, false negative events occurred when the vehicles were positioned further away from the LiDAR (Scene B). The bounding box regression results seem inaccurate for the single-unit trucks (Scene D) since this type of truck is under-represented in the nuScene dataset. Similarly, tractor-trailer trucks and straight trucks with a trailer were commonly identified as two separate vehicles due to the dissimilar population between the training and testing set. Therefore, this preliminary analysis concluded that the pre-trained PointPillar needs to be fine-tuned to better adapt to the task of truck detection and classification in the future.

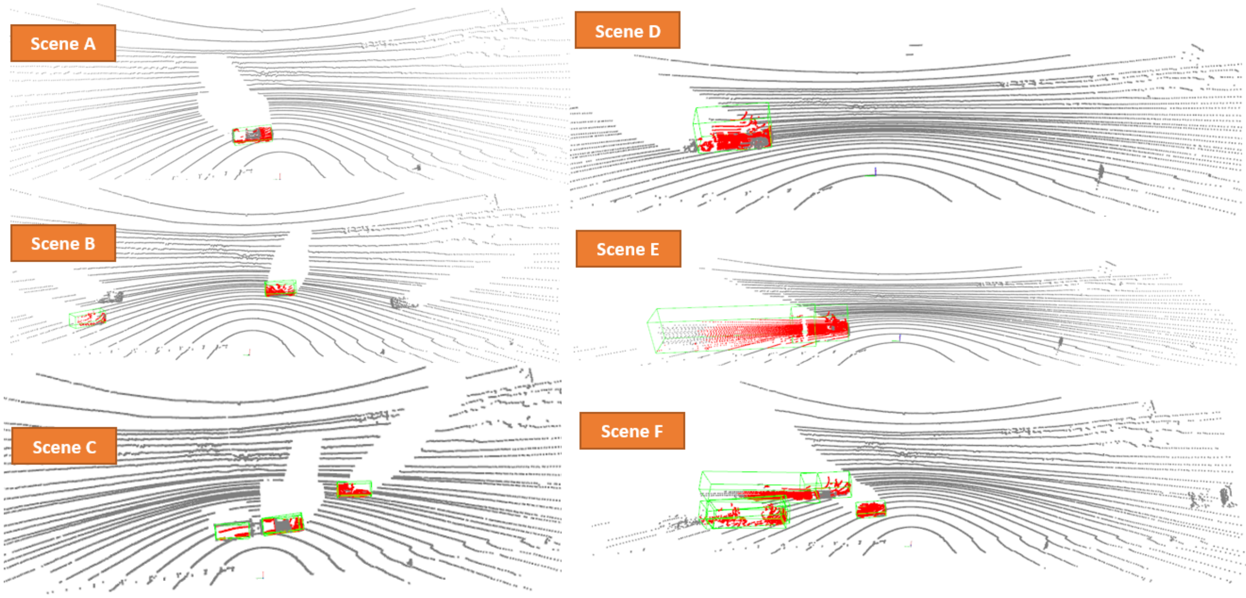

Figure 4-5 PointPillar Detection Results

Chapter 5 Microscopic Trajectory Estimation using LiDAR

5.1 Introduction

The microscopic trajectory of a vehicle consists of information about its position at discrete timesteps over a defined time interval. Given such trajectory, vehicle's instantaneous speed, acceleration, deceleration, and other traffic state parameters can be derived(*28*). Such microscopic characteristics are necessary for better traffic operations. Microscopic trajectories are used to study and understand various traffic flow phenomena like car-following behavior, lane changing behavior, capacity drop, traffic oscillation propagation, calibrating and validating car-following models, and traffic simulation models close to real world(*29*–*31*). These trajectories are also very important to be able to assess traffic safety by means of conforming to the speed limits and maintaining reasonable headways as well as lane positions. Surrogate safety measures (SSM) are widely used important metrics to assess traffic safety and use vehicle trajectories and interaction between vehicles to estimate SSM metrics(*32*, *33*). They are also very important input for microscopic emission models such as Comprehensive Model Emissions Model (CMEM) and Motor Vehicle Emissions Simulator (MOVES) as they consider comprehensive modeling framework for driving behavior(*34*, *35*). In this chapter we focus on estimating the microscopic trajectories of each vehicle using Light Detection and Ranging (LiDAR), an active remote sensing technique.

LiDAR emits near infrared light and collects information about the geometry and reflectivity of the target environment. For the current study, a 32 beam LiDAR sensor rotating 180 degrees in the horizontal field of view is used. The raw point clouds obtained from the Lidar are processed to remove background using DBSCAN, and statistical outliers as proposed in (*36*). Each scan of the side-fire Lidar sensor captures all the truck bodies present in its Detection Zone (LDZ) partially. The scan will have rich information of the front portion of the truck when it is entering the LDZ, the side of the truck when it is in the midsection part of the LDZ and the rear portion of the vehicle when it is leaving the LDZ as shown in Figure 5-1 below.

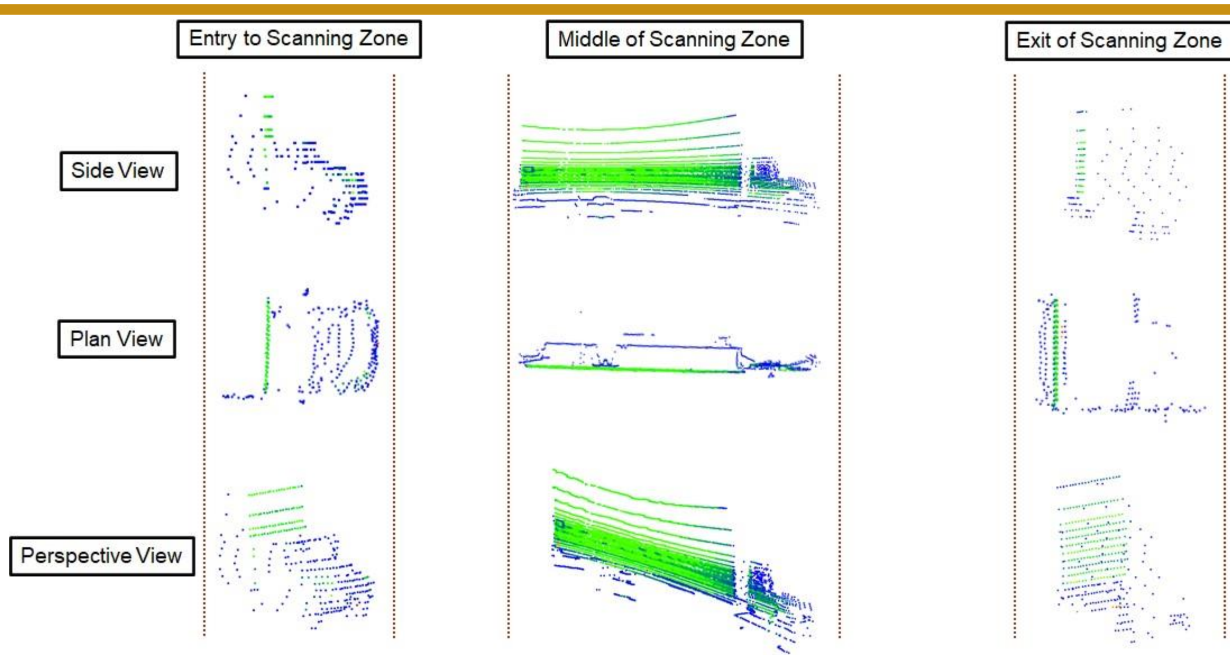

Figure 5-1 Point Clouds representing individual scans of vehicles at various sections of LiDAR Detection Zone (LDZ)

Trajectories of the vehicles passing through the LDZ can be estimated using data association and tracking of the same reference point on the corresponding raw scans of a vehicle. This reference can be a corner point of a minimum bounding box or the centroid of the bounding box either in 2D or 3D. Such an attempt has been made using the centroid of a 2D bounding box of individual scans for the purpose of truck body reconstruction in (*37*). One drawback of this approach to be used for trajectory estimation is the inherent shift in the centroid of the bounding box in successive scans ascribed to the varying size of the vehicle's point cloud as it passes through the LDZ.

When the vehicle is passing through the entry zone of the LDZ, size (length) of the point cloud grows in each successive scan as it progressively captures more and more rear part of the vehicle until it reaches the mid zone of the LDZ. Due to this, the estimated centroid in each successive scan is closer to the previous centroid than it should be. Similarly, as the vehicle leaves the LDZ from midsection, each successive scan progressively loses the front portion of the vehicle. This also results in the centroids in the exit zone being closer than they should have been. Speed estimated from such trajectories would be an underestimation in the entry and exit zones of the LDZ. This necessitates an alternative approach which can overcome the error due to the partial nature of the raw point clouds. To overcome the above stated drawbacks, we proposed a forward – backward pass rigid body transformation-based approach for estimating accurate microscopic trajectories. During the forward pass, the entire scanned body of the vehicle is reconstructed using pairwise registration. The centroid of the minimum bounding box for such a reconstructed vehicle is very close to the actual centroid of the vehicle. This fully reconstructed vehicle is projected backward to each individual scan using inverse transformation during the backward pass. The trajectory of the vehicle is estimated using the centroid of the bounding box for these fully reconstructed vehicles. Such high temporal resolution trajectories have immense potential for further use in accurate emission estimates, traffic state estimates and traffic safety applications.

5.2 Literature Review of Related Work

5.2.1 Trajectory Estimation

Microscopic vehicle trajectories are critical data for understanding car-following behavior, lane changing behavior and gap acceptance, which are core inputs for developing and advancing traffic flow theory, which in turn have impact on planning and operations of transport facilities. Understanding this Federal Highway(*38*). With the advances in communication and information technologies these trajectories are obtained by a variety of sensing technologies such as video-based image processing(*29*–*31*), global positioning systems (GPS), location-based services such as cellular networks, wireless fidelity (WiFi), Bluetooth based probes, license plates(*39*), and probe vehicles(*40*).

Except video-based image techniques, all other methods provide spatially sparse trajectories known as macro trajectories. There are methods proposed to derive microtrajectories from probe vehicle-based macro trajectories in the literature(*41*, *42*). Trajectories estimated from these existing Intelligent Transportation System sensors have uses as well as limitations. Sometimes it takes a long time to identify shortcomings of such data, as happened in the case of the Next Generation Simulation (NGSIM) dataset collected during mid-2000s. Authors caution that without accurate empirical microscopic trajectories, “plausible but inaccurate hypotheses perpetuate in vacuum(*38*).” Also, video cameras which are only able to provide microscopic trajectories in the field of vision, have difficulty to operate efficiently under all lighting conditions. Light Detection and Ranging (LiDAR), an active remote sensing technology, has the potential to overcome these shortcomings and be able to provide accurate microscopic trajectories due to its nature of providing three dimensional measurements of the target environment(*43*). LiDAR is used as a key sensor to detect and track objects in autonomous driving (*44*) and paved the way forward for it being tested as an infrastructure-based traffic sensing device, especially from the connected vehicles (CV) perspective especially to get microscopic traffic states of vehicles not equipped with CV capabilities(*45*–*47*). As part of this effort researchers have proposed roadside LiDAR based microscopic trajectory estimation frameworks. Sun, Y et al. (2018) proposed a framework to extract vehicle trajectories from the 3-D LiDAR data. Their framework consists of raw data processing; statistical outlier removal of noise points; RANSAC algorithm-based ground plane segmentation to eliminate the points corresponding to road surface; basic clustering techniques-based algorithm to cluster points of individual vehicles; principal component analysis (PCA) based oriented bounding box (OBB) estimation for the vehicles and geometry-based tracking algorithm. In this study the OBB’s front right corner was used for tracking the vehicle while approaching the LiDAR sensor, and the rear right corner of the OBB was used while the vehicle was departing the LiDAR sensor. One of the key findings while evaluating this framework was that the estimated speed of the vehicle may suddenly drop or increase. This is attributable to the effect of using the OBB of individual partial scans(*48*).

Other frameworks proposed mainly in the context of tracking road users like vehicles and pedestrians have similar steps of LiDAR raw data processing, background elimination, clustering of individual road users, classification of road users, tracking the road users using variants of Kalman Filter(*45*, *46*, *49*). All these studies track individual road users with the help of a selected reference point on their oriented bounding box like centroid, right corner, left corner. One thing in common for all these studies is using the bounding box of individual LiDAR scans, which results in sharp increase or decrease of the speed.

Zhang, J et al., (2019) proposed a refined tracking process using the images of LiDAR scans. In this study, a maximum distance-based background filter mask gives the moving LiDAR points of road users. Individual road users are identified using a Euclidean distance-based clustering technique. A SVM binary classifier separates vehicles from non-vehicles. They proposed an image based two-stage tracking step to overcome the bias induced due to incompleteness of individual scans. In the first stage, pairwise registration of individual LiDAR scan images is carried-out with respect to the LiDAR image of first scan to build a reference image by combining all scans. In the second stage, this reference image is invert transformed back to each of the individual scans. The centroid of the reference image in these new positions defines the trajectory of the vehicle. One major limitation of this approach is that every LiDAR scan image should have an overlapping region with respect to the first scan image for getting an accurate image registration result. This would shorten the length of the estimated vehicle trajectory. Another limitation of this approach is the warping LiDAR images would undergo during horizontal curve maneuvers, which might further reduce the length of the trajectory. Another disadvantage is losing the rich third dimensional data of the LiDAR sensor.

To overcome the above mentioned shortcomings, we investigated a forward – backward pass framework for estimating microscopic trajectories using LiDAR point clouds. The rest of the chapter is organized as mentioned here. The next section discusses the data collection set up at SR-7, Calexico in Southern California. The subsequent section discusses the detailed steps of the methodology framework we proposed. The last section discusses the results and future work.

5.3 Data Collection Setup

LiDAR data is collected on state route SR-7 (Figure 5-2) south of state route SR-98 at Calexico in the state of California. The data collection site has an intersection downstream of the LiDAR sensor, increasing the chance of observing lane change phenomena.

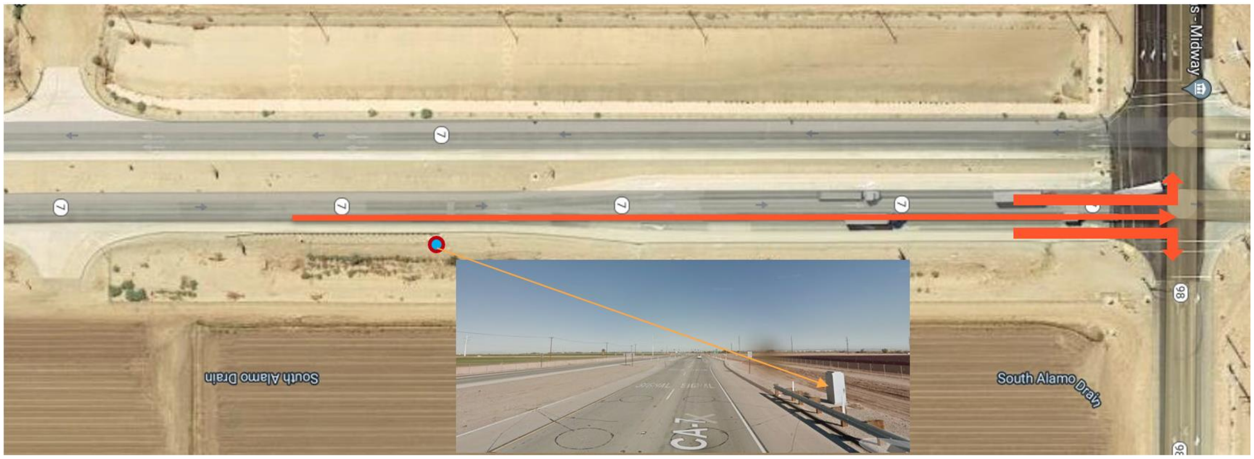

Figure 5-2. LiDAR data collection site at Calexico

5.4 Methodology

The proposed methodology consists of processing raw LiDAR data collected through three steps. The first step involves background elimination during which all non-vehicular points are removed from the captured LiDAR data. For this purpose, a threshold-based mask filter for spatial occupancy of points is used to eliminate the background. Once the background is eliminated, the DBSCAN clustering algorithm is used for identifying all individual vehicles present in the LDZ. Once all individual vehicle points in each successive scan are collected for the duration of the data collection period, it is important to group all the LiDAR scans of each single vehicle. A Global Nearest Neighbor (GNN) and Hungarian Algorithm based data association in combination with Kalman Filter based tracking is used to establish collection of all LiDAR scans for every single vehicle that passed through the LDZ. All these three steps are explained in Li, Y et al. (*36*).

While a trajectory for the vehicle can be established during the third step mentioned earlier, it is limited in accuracy due to the following explanation. As the vehicle is passing through the LDZ, only its partial body gets scanned and is continuously varying in size. The scanned part of the vehicle's body increases in size from the beginning until mid-portion and starts decreasing after this. This is illustrated in Figure 5-3 below. Also, we can note that the vehicle scans at the entry and exit have a very small number of points. This induces errors in the trajectory being obtained during the tracking stage. To overcome this, a forward-backward pass approach is adopted for estimating accurate trajectories of the vehicle passing through the LDZ.

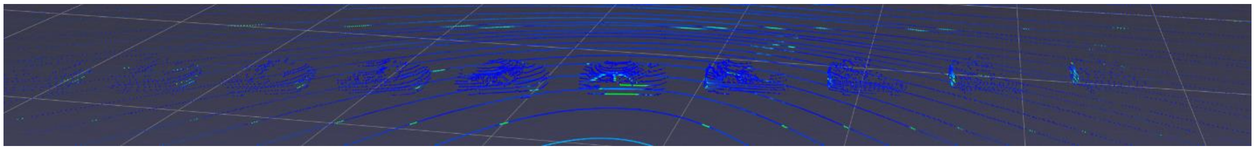

Figure 5-3. Raw LiDAR scans of vehicle while passing through LDZ

5.4.1 Identification of suitable registration pipeline for LiDAR point clouds

Identification of a robust registration pipeline combining the available registration algorithms is extremely important for the trajectory estimation purposes. The earlier registration pipeline established by Allu, et al. (*37*) does not take road plane constraint into account. Another pipeline is established by Li, Y et al.(*50*) but excludes the LiDAR scans in the beginning and end parts of the LDZ. Hence it is necessary to determine a robust registration pipeline from the beginning to the end of the LDZ quantitatively.

5.4.2 Determination of Optimal Registration Pipeline

Identification of a robust registration pipeline with a combination of existing algorithms such that it works accurately across the entire LiDAR Detection Zone is very important. This ensures an accurate microscopic trajectory of the vehicle as well.

To identify an accurate registration pipeline, a quantitative simulation experiment is setup as follows. For every 'i^{th}' frame(scan) of the vehicle which acts as a source, a target point cloud is created by subjecting it to a known rotation of 10 degrees around the Z-axis in the road plane and a translation of 0.5m and 1.0m in X and Y-axis directions, respectively. A set of six registration pipelines are chosen based on literature review and the works carried out in (*37*, *50*). These pipelines are illustrated in Figure 5-4.

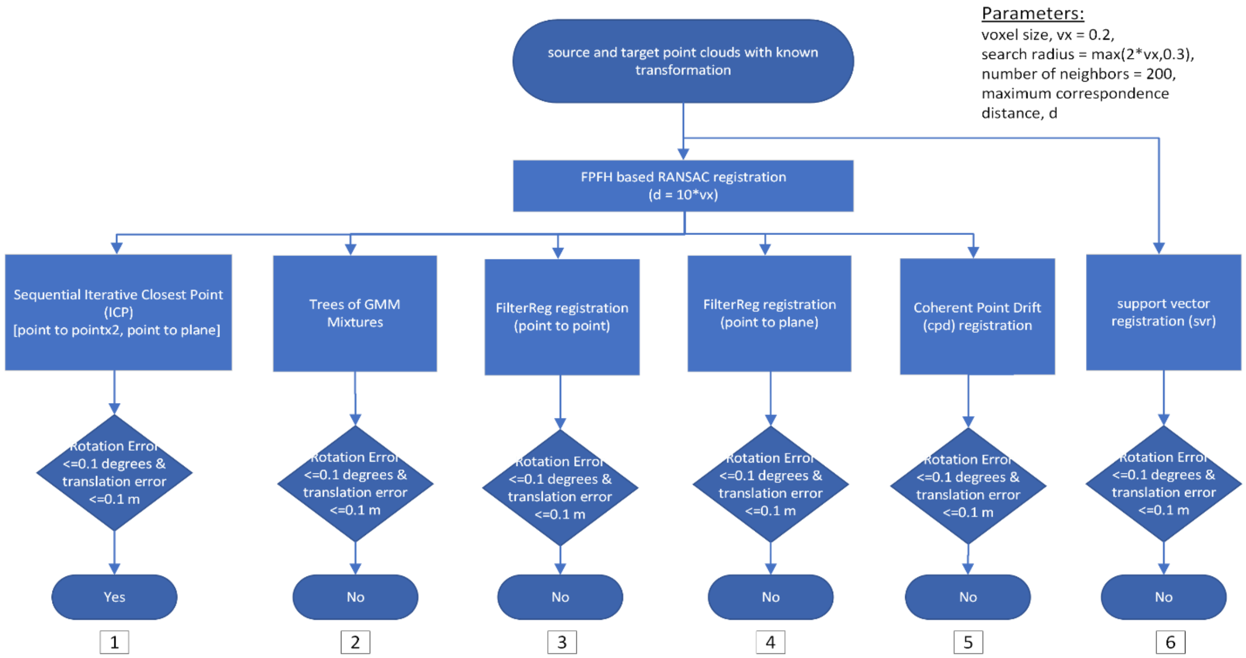

Figure 5-4. Set of Registration pipelines evaluated

The proposed set of pipelines are tested to verify if it can estimate the ‘known induced’ rotation and translation accurately between each of these source and target pairs. The absolute error between induced and estimated rotations as well as translations is used to choose the appropriate registration pipeline for further use. The results of the experiment are shown in the plot presented as Figure 5-5 below.

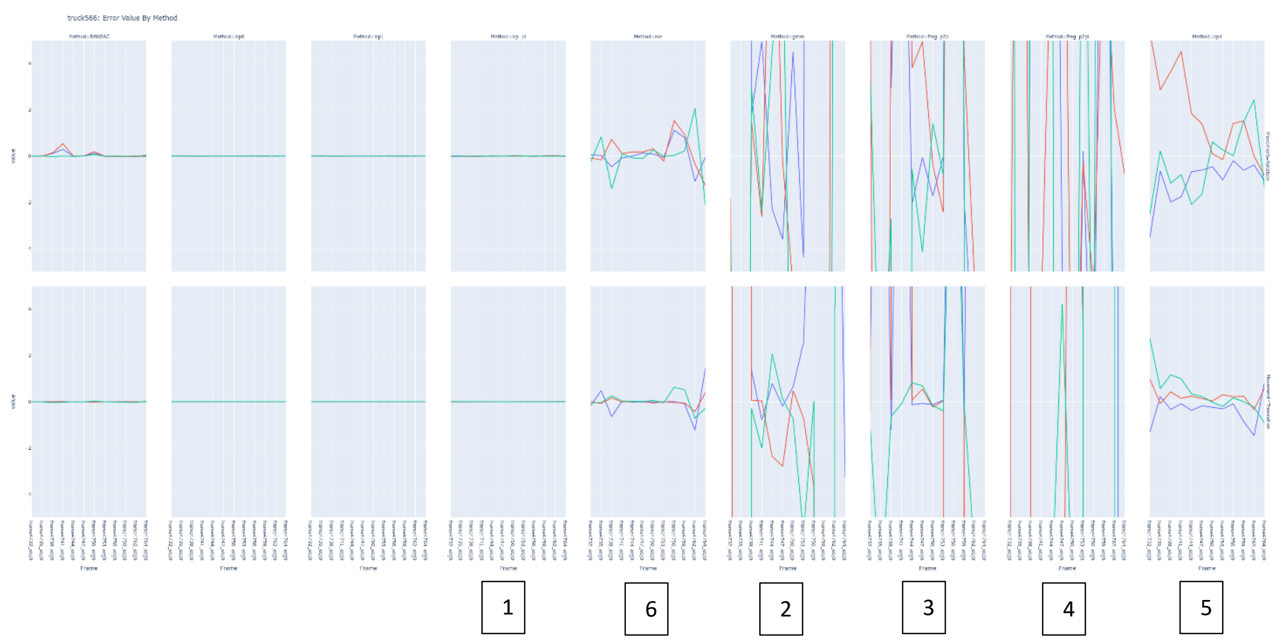

Figure 5-5. Absolute Error between induced and estimated rotation, translations

Except the registration pipeline number 1, other pipelines did not estimate the induced transformation accurately enough. Hence the first pipeline would be used in the further steps of truck reconstruction.

5.4.3 Microscopic Trajectory Estimation

The registration pipeline chosen in the previous section is shown in Figure 5-6. This optimal pairwise registration (OPR) pipeline is used to estimate the pairwise rigid body transformation matrices between successive scans of a vehicle. For each of these transformation matrices the corresponding quality metrics fitness and RMSE values are also stored.

The fitness and RMSE values of the pairwise registration indicate its accuracy. A high fitness score and low RMSE values are desirable, and from the experimental setup of registration pipelines a fitness score above 0.98 and RMSE value less than 0.2 indicate a good pairwise registration. Even though the registration pipeline is chosen based upon quantitative accuracy, the values of these metrics does not always comply to the accuracy threshold values. This can be seen in Figure 5-7 below. The example showcased is a truck which has 86 lidar scans. There are a total of 9 discontinuities where OPR did not result in expected accuracy. A qualitative investigation of these breakdowns can be done using Figure 5-8. Figure 5-8 showcases partial reconstructions of the truck where OPR values are continuously accurate.

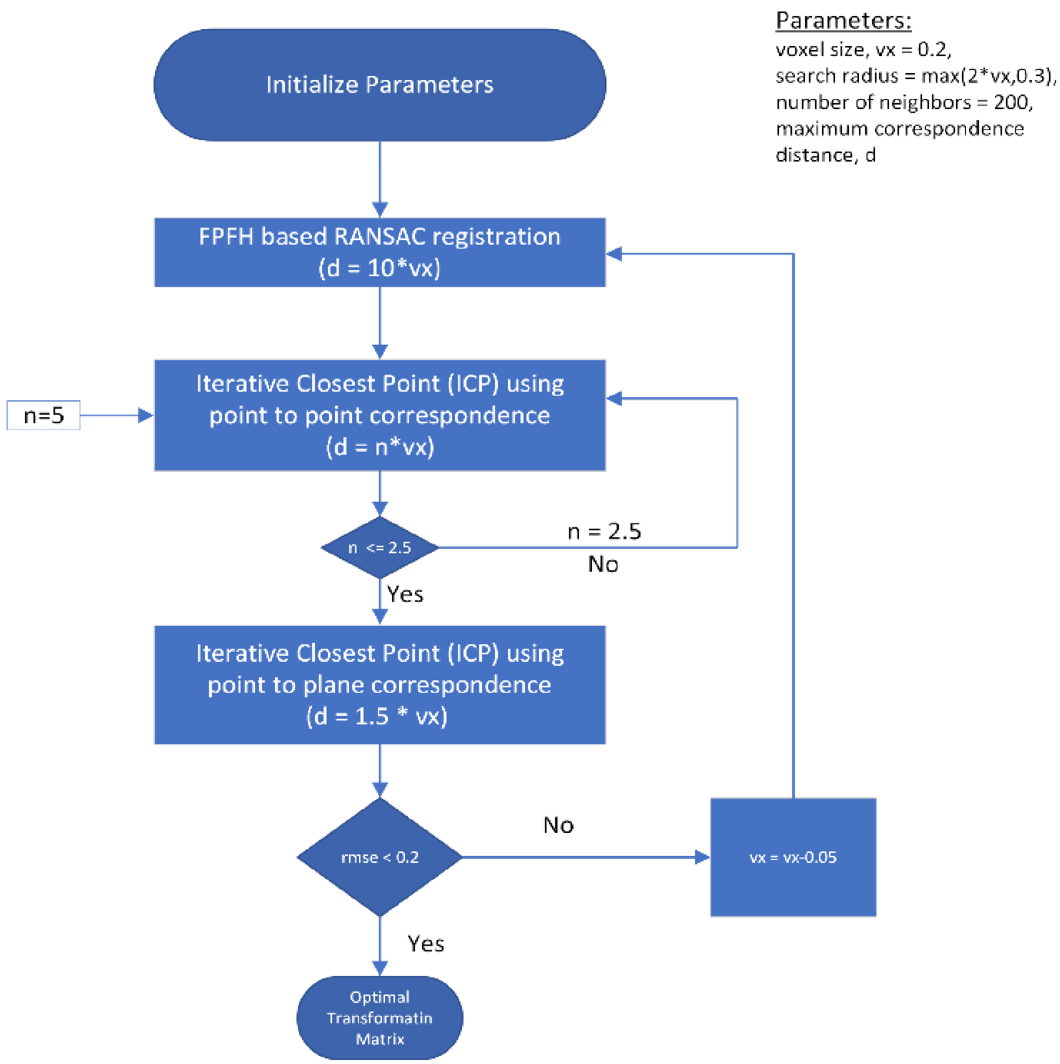

Figure 5-6. Optimal Pairwise Registration Pipeline

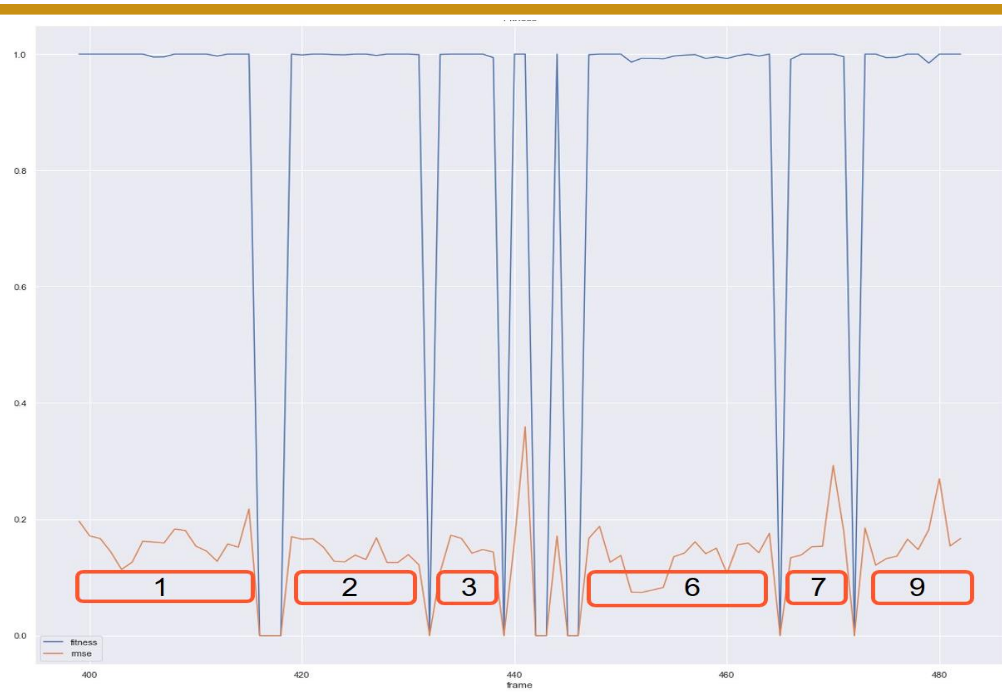

Figure 5-7. Fitness and RMSE values of OPR for a truck

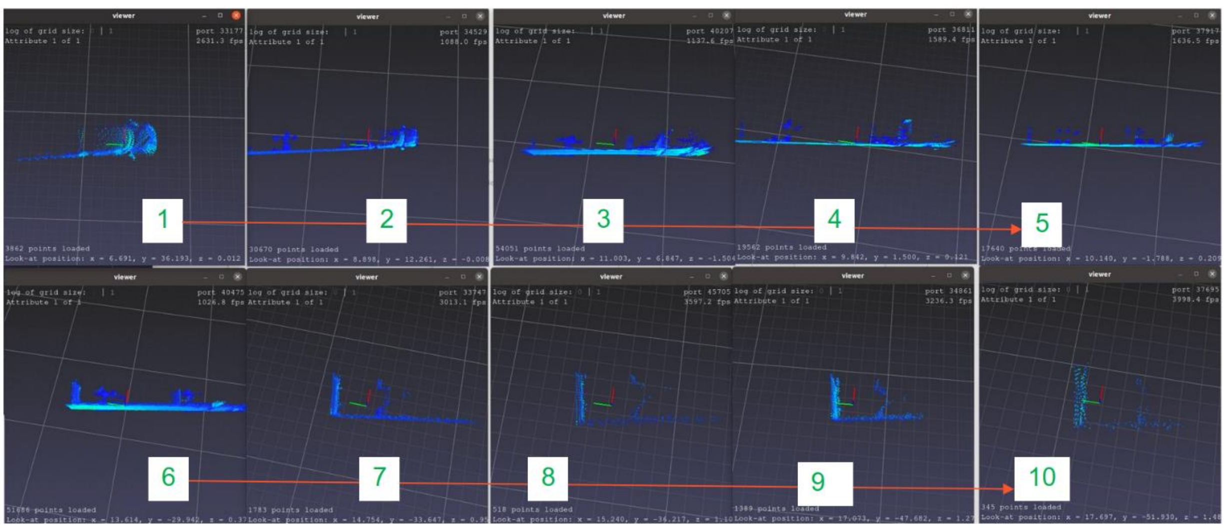

Figure 5-8. Visual Investigation of OPR breakdowns

Visual investigation of the discontinuities revealed why OPR was not doing well at those discontinuities. These lucid observations are presented in Table 5-1 below.

Table 5-1. Analysis of OPR discontinuities

Discontinuity	Explanation
Between 1 and 2	The front vertical surface of the trailer appears at greater detail compared to the scans before causing the discontinuity.
Between 2 and 3	The vertical surface of the trailer is not scanned as the truck is almost perpendicular to the LiDAR in this portion, and this information has been lost compared to previous scans.
Between 3 and 4	The rear vertical surface of the cab starts appearing in greater detail compared to the previous scans causing the breakdown.
Between 4 and 5	The rear vertical surface is completely obscured by the side vertical face of the trailer, and this information is missing compared to the previous scans.
Between 5 and 6	The rear vertical surface of the trailer is more pronounced in the 6th partial reconstruction compared to the 5th.
Between 6 and 7	The Cab information is completely lost in the 7th, and only half of the trailer is present compared to 6th.
Between 7 and 8	Further breakdowns happened due to the slow disappearance of the trailer's side face and rear axle.

To overcome this shortcoming of the OPR, adjacent partially reconstructed point clouds were used to obtain the transformation matrices at the discontinuities. The entire scanned body of the vehicle passing through the LDZ was reconstructed after all transformation matrices were obtained. The microscopic trajectory of the vehicle was obtained by performing sequential inverse rigid body transformations of the reconstructed vehicle body. The total flow of tasks involved in microscopic trajectory estimation are presented in Figure 5-9. An example trajectory of a truck passing through the LDZ is presented in Figure 5-10. A lane change captured at the beginning of the trajectory can also be observed.

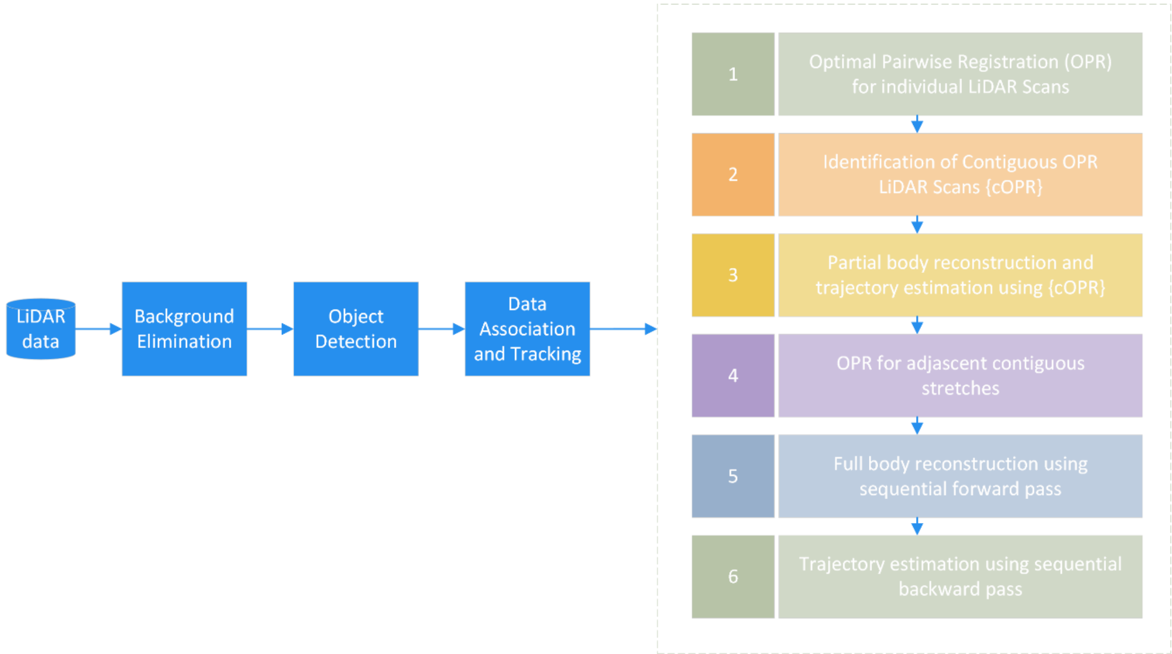

Figure 5-9. Total workflow of Microscopic Trajectory Estimation

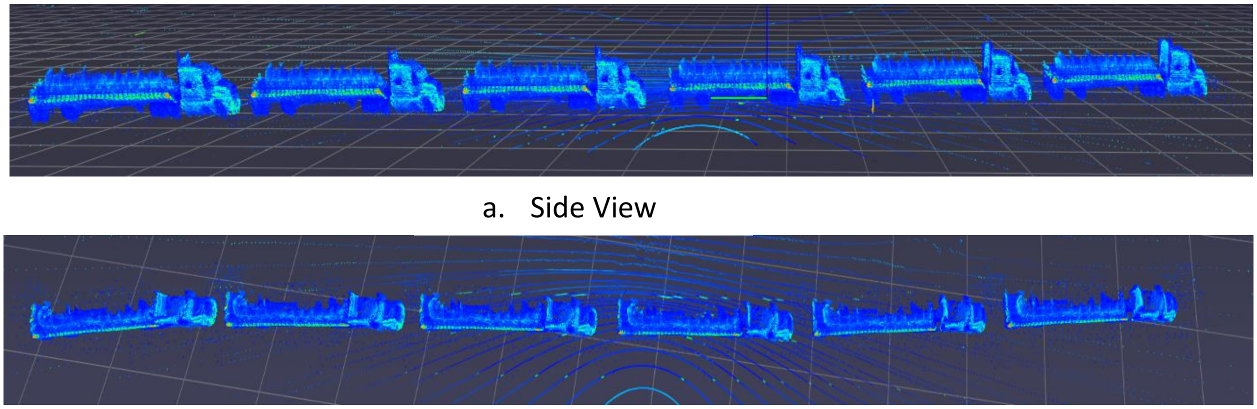

a. Side View

b. Top View

Figure 5-10. An Example of Microscopic Trajectory presented at 1 second aggregation from reconstructed LiDAR scans

5.5 Analysis and Discussion

For preliminary analysis, the trajectory of the passing truck is estimated as the centroid of a 2D bounding box projected on to the road plane. Also, vehicle speed, acceleration and change in travel direction are estimated using the trajectory.

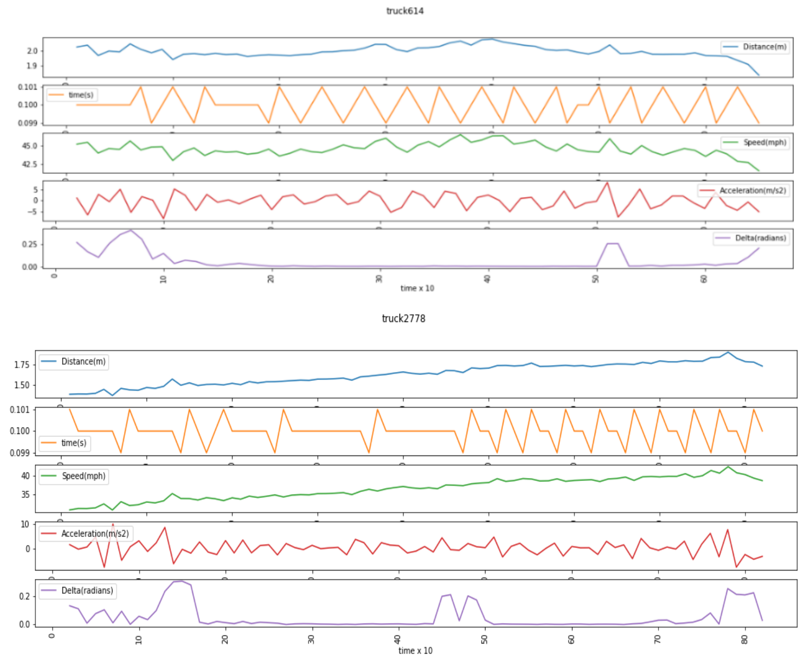

Figure 5-11. Few examples of Trajectories and corresponding traffic characteristics of the Trucks

These plots show that detailed microscopic trajectories can be estimated with the proposed framework.

Microscopic trajectories of vehicles have potential to address well known challenges such as calibrating and validating microscopic traffic flow models, estimating surrogate safety measures, and estimating microscopic emissions and energy. They also have promise to contribute and draw insights to better understand emerging transportation systems such as connected and automated vehicles and coordinated driving strategies as part of achieving efficient electric grid-mobility integrations, etc.

In this chapter, we developed a forward-backward pass microscopic trajectory estimation framework for a LiDAR sensor that can potentially address the bias of using individual scan-based tracking. A major contribution of this framework is development of a multistage coarse-to-fine pairwise rigid body registration pipeline to achieve accurate transformation matrices throughout the LiDAR detection zone, which overcame the limitations of approaches that excluded LiDAR scans from the entry and exit portions of the detection zone. The proposed framework extended the length over which a vehicle can be tracked and in turn the length of microscopic trajectories.

References

1. Romero, A. ROS Concepts. http://wiki.ros.org/ROS/Concepts. Accessed Sep. 10, 2022.

2. Lee, H., and B. Coifman. Side-Fire Lidar-Based Vehicle Classification. *Transportation Research Record*, No. 2308, 2012, pp. 173–183. https://doi.org/10.3141/2308-19.

3. Zhang, Z. Y., J. Zheng, X. Wang, and X. Fan. Background Filtering and Vehicle Detection with Roadside Lidar Based on Point Association. *Chinese Control Conference, CCC*, Vol. 2018-July, 2018, pp. 7938–7943. https://doi.org/10.23919/ChiCC.2018.8484040.

4. Zhang, Z., J. Zheng, H. Xu, and X. Wang. Vehicle Detection and Tracking in Complex Traffic Circumstances with Roadside LiDAR. *Transportation Research Record*, Vol. 2673, No. 9, 2019, pp. 62–71. https://doi.org/10.1177/0361198119844457.

5. Zhang, J., W. Xiao, B. Coifman, J. P. Mills, Z. Y. Zhang, J. Zheng, H. Xu, X. Wang, H. Lee, B. Coifman, J. Zhao, H. Xu, H. Liu, J. Wu, Y. Zheng, D. Wu, H. Xu, J. Zheng, Z. Y. Zhang, J. Zheng, X. Wang, and X. Fan. Vehicle Tracking and Speed Estimation from Roadside Lidar. *Transportation Research Record*, Vol. 13, No. 9, 2019, pp. 173–183. https://doi.org/10.23919/ChiCC.2018.8484040.

6. Wu, J., H. Xu, and J. Zheng. Automatic Background Filtering and Lane Identification with Roadside LiDAR Data. *IEEE Conference on Intelligent Transportation Systems, Proceedings, ITSC*, Vol. 2018-March, 2018, pp. 1–6. https://doi.org/10.1109/ITSC.2017.8317723.

7. Lv, B., H. Xu, J. Wu, Y. Tian, and C. Yuan. Raster-Based Background Filtering for Roadside LiDAR Data. *IEEE Access*, Vol. 7, 2019, pp. 76779–76788. https://doi.org/10.1109/ACCESS.2019.2919624.

8. Zhao, J., H. Xu, X. Xia, and H. Liu. Azimuth-Height Background Filtering Method for Roadside LiDAR Data. *2019 IEEE Intelligent Transportation Systems Conference, ITSC 2019*, 2019, pp. 2421–2426. https://doi.org/10.1109/ITSC.2019.8917369.

9. Zhang, T., and P. J. Jin. Roadside LiDAR Vehicle Detection and Tracking Using Range and Intensity Background Subtraction. *Journal of Advanced Transportation*, Vol. 2022, No. Cv, 2022. https://doi.org/10.1155/2022/2771085.

10. Dai, J., Y. Li, K. He, and J. Sun. R-FCN: Object Detection via Region-Based Fully Convolutional Networks. *Advances in Neural Information Processing Systems*, 2016, pp. 379–387.

11. Girshick, R., J. Donahue, T. Darrell, and J. Malik. Rich Feature Hierarchies for Accurate Object Detection and Semantic Segmentation. *Proceedings of the IEEE Computer Society Conference on Computer Vision and Pattern Recognition*, 2014, pp. 580–587. https://doi.org/10.1109/CVPR.2014.81.

12. Ren, S., K. He, R. Girshick, and J. Sun. Faster R-CNN: Towards Real-Time Object Detection with Region Proposal Networks. *IEEE Transactions on Pattern Analysis and Machine Intelligence*, Vol. 39, No. 6, 2017, pp. 1137–1149. https://doi.org/10.1109/TPAMI.2016.2577031.

13. Liu, W., D. Anguelov, D. Erhan, C. Szegedy, S. Reed, C. Y. Fu, and A. C. Berg. SSD: Single Shot Multibox Detector. *Lecture Notes in Computer Science (including subseries Lecture Notes in Artificial Intelligence and Lecture Notes in Bioinformatics)*, Vol. 9905 LNCS, 2016, pp. 21–37. https://doi.org/10.1007/978-3-319-46448-0_2.

14. Redmon, J., S. Divvala, R. Girshick, and A. Farhadi. You Only Look Once: Unified, Real-Time Object Detection. *Proceedings of the IEEE Computer Society Conference on Computer Vision and Pattern Recognition*, Vol. 2016-Decem, 2016, pp. 779–788. https://doi.org/10.1109/CVPR.2016.91.

15. Li, B., T. Zhang, and T. Xia. Vehicle Detection from 3D Lidar Using Fully Convolutional Network. *Robotics: Science and Systems*, Vol. 12, 2016. https://doi.org/10.15607/rss.2016.xii.042.

16. Tran, D., L. Bourdev, R. Fergus, L. Torresani, and M. Paluri. Learning Spatiotemporal Features with 3D Convolutional Networks. 2014.

17. Yang, B., W. Luo, and R. Urtasun. PIXOR: Real-Time 3D Object Detection from Point Clouds. *Proceedings of the IEEE Computer Society Conference on Computer Vision and Pattern Recognition*, 2018, pp. 7652–7660. https://doi.org/10.1109/CVPR.2018.00798.

18. Lang, A. H., S. Vora, H. Caesar, L. Zhou, J. Yang, and O. Beijbom. Pointpillars: Fast Encoders for Object Detection from Point Clouds. *Proceedings of the IEEE Computer Society Conference on Computer Vision and Pattern Recognition*, Vol. 2019-June, 2019, pp. 12689–12697. https://doi.org/10.1109/CVPR.2019.01298.

19. Qi, C. R., H. Su, K. Mo, and L. J. Guibas. PointNet: Deep Learning on Point Sets for 3D Classification and Segmentation. *Proceedings - 30th IEEE*

Conference on Computer Vision and Pattern Recognition, CVPR 2017, Vol. 2017-Janua, 2017, pp. 77–85. https://doi.org/10.1109/CVPR.2017.16.

20. Asvadi, A., L. Garrote, C. Premebida, P. Peixoto, and U. J. Nunes. DepthCN: Vehicle Detection Using 3D-LIDAR and ConvNet. *IEEE Conference on Intelligent Transportation Systems, Proceedings, ITSC*, Vol. 2018-March, 2018, pp. 1–6. https://doi.org/10.1109/ITSC.2017.8317880.

21. Chen, X., H. Ma, J. Wan, B. Li, and T. Xia. Multi-View 3D Object Detection Network for Autonomous Driving. *Proceedings - 30th IEEE Conference on Computer Vision and Pattern Recognition, CVPR 2017*, Vol. 2017-Janua, 2017, pp. 6526–6534. https://doi.org/10.1109/CVPR.2017.691.

22. Shi, S., X. Wang, and H. Li. PointRCNN: 3D Object Proposal Generation and Detection from Point Cloud. *Proceedings of the IEEE Computer Society Conference on Computer Vision and Pattern Recognition*, Vol. 2019-June, 2019, pp. 770–779. https://doi.org/10.1109/CVPR.2019.00086.

23. Ettinger, S., S. Cheng, B. Caine, C. Liu, H. Zhao, S. Pradhan, Y. Chai, B. Sapp, C. Qi, Y. Zhou, Z. Yang, A. Chouard, P. Sun, J. Ngiam, V. Vasudevan, A. McCauley, J. Shlens, and D. Anguelov. Large Scale Interactive Motion Forecasting for Autonomous Driving: The WAYMO OPEN MOTION DATASET. *Proceedings of the IEEE International Conference on Computer Vision*, 2021, pp. 9690–9699. https://doi.org/10.1109/ICCV48922.2021.00957.

24. Houston, J., G. Zuidhof, L. Bergamini, Y. Ye, L. Chen, A. Jain, S. Omari, V. Iglovikov, and P. Ondruska. One Thousand and One Hours: Self-Driving Motion Prediction Dataset. No. CoRL 2020, 2020, pp. 1–10.

25. Geiger, A., P. Lenz, C. Stiller, and R. Urtasun. Vision Meets Robotics: The KITTI Dataset. The International Journal of Robotics Research. *The International Journal of Robotics Research*, No. October, 2013, pp. 1–6.

26. Caesar, H., V. Bankiti, A. H. Lang, S. Vora, V. E. Liong, Q. Xu, A. Krishnan, Y. Pan, G. Baldan, and O. Beijbom. Nuscenes: A Multimodal Dataset for Autonomous Driving. *Proceedings of the IEEE Computer Society Conference on Computer Vision and Pattern Recognition*, No. March, 2020, pp. 11618–11628. https://doi.org/10.1109/CVPR42600.2020.01164.

27. Foley, J. D., M. A. Fischler, and R. C. Bolles. *Graphics and Image Processing Random Sample Consensus: A Paradigm for Model Fitting with Apphcatlons to Image Analysis and Automated Cartography*. 1981.

28. Pal, D., and M. Chunchu. Smoothing of Vehicular Trajectories under Heterogeneous Traffic Conditions to Extract Microscopic Data. *Canadian Journal of Civil Engineering*, Vol. 45, No. 6, 2018, pp. 435–445.

29. Kovvali, V. G., V. Alexiadis, and Z. Lin. Video-Based Vehicle Trajectory Data Collection. 2006.

30. Anagnostopoulos, A., and F. Kehagia. Utilizing UAVs Technology on Microscopic Traffic Naturalistic Data Acquirement. *Infrastructures*, Vol. 6, 2021, p. 89. https://doi.org/10.3390/infrastructures6060089.

31. Shi, X., D. Zhao, H. Yao, X. Li, D. K. Hale, and A. Ghiasi. Video-Based Trajectory Extraction with Deep Learning for High-Granularity Highway Simulation (HIGH-SIM). *Communications in Transportation Research*, Vol. 1, 2021, p. 100014. https://doi.org/10.1016/J.COMMTR.2021.100014.

32. Nour, M. W. Monitoring of Microscopic Traffic Behavior for Safety Applications Using Temporal Logic. *Electronic Theses and Dissertations, 2020-*, 2021.

33. Wang, C., Y. Xie, H. Huang, and P. Liu. A Review of Surrogate Safety Measures and Their Applications in Connected and Automated Vehicles Safety Modeling. *Accident Analysis & Prevention*, Vol. 157, 2021, p. 106157. https://doi.org/10.1016/J.AAP.2021.106157.

34. Shan, X., P. Hao, X. Chen, K. Boriboonsomsin, G. Wu, and M. J. Barth. Vehicle Energy/Emissions Estimation Based on Vehicle Trajectory Reconstruction Using Sparse Mobile Sensor Data. *IEEE Transactions on Intelligent Transportation Systems*, Vol. 20, No. 2, 2019, pp. 716–726. https://doi.org/10.1109/TITS.2018.2826571.

35. Tsanakas, N., J. Ekström, and J. Olstam. Generating Virtual Vehicle Trajectories for the Estimation of Emissions and Fuel Consumption. *Transportation Research Part C: Emerging Technologies*, Vol. 138, 2022, p. 103615. https://doi.org/10.1016/J.TRC.2022.103615.

36. Li, Y., K. R. Allu, Z. Sun, A. Y. C. Tok, G. Feng, and S. G. Ritchie. Truck Body Type Classification Using a Deep Representation Learning Ensemble on 3D Point Sets. *Transportation Research Part C: Emerging Technologies*, Vol. 133, 2021, p. 103461. https://doi.org/10.1016/J.TRC.2021.103461.

37. Allu, K. R., Z. Sun, and A. Tok. *Lidar Based Reconstruction Framework for Truck Surveillance*. 2020.

38. Coifman, B., and L. Li. A Critical Evaluation of the Next Generation Simulation (NGSIM) Vehicle Trajectory Dataset. *Transportation Research*

Part B: Methodological, Vol. 105, 2017, pp. 362–377. https://doi.org/10.1016/J.TRB.2017.09.018.

39. Zhang, Z., H. Liu, L. Rai, and S. Zhang. Vehicle Trajectory Prediction Method Based on License Plate Information Obtained from Video-Imaging Detectors in Urban Road Environment. *Sensors 2020, Vol. 20, Page 1258*, Vol. 20, No. 5, 2020, p. 1258. https://doi.org/10.3390/S20051258.

40. Yao, Z., M. Liu, Y. Jiang, Y. Tang, and B. Ran. Trajectory Reconstruction for Mixed Traffic Flow with Regular, Connected, and Connected Automated Vehicles on Freeway. *IET Intelligent Transport Systems*, 2022. https://doi.org/10.1049/ITR2.12294.

41. Coifman, B., M. Wu, K. Redmill, and D. A. Thornton. Collecting Ambient Vehicle Trajectories from an Instrumented Probe Vehicle: High Quality Data for Microscopic Traffic Flow Studies. *Transportation Research Part C: Emerging Technologies*, Vol. 72, 2016, pp. 254–271. https://doi.org/10.1016/J.TRC.2016.09.001.

42. Li, Y., S. Chen, R. Du, P. Ha, J. Dong, and S. Labi Professor. Using Empirical Trajectory Data to Design Connected Autonomous Vehicle Controllers for Traffic Stabilization.

43. Barad, J. *Roadside Lidar Helping to Build Smart and Safe Transportation Infrastructure*. SAE Technical Paper, 2021.

44. Luo, Z., S. Habibi, and M. V Mohrenschildt. LiDAR Based Real Time Multiple Vehicle Detection and Tracking.

45. Chen, J., S. Tian, H. Xu, R. Yue, Y. Sun, and Y. Cui. Architecture of Vehicle Trajectories Extraction with Roadside Lidar Serving Connected Vehicles. *IEEE Access*, Vol. 7, 2019, pp. 100406–100415. https://doi.org/10.1109/ACCESS.2019.2929795.

46. Cui, Y., H. Xu, J. Wu, Y. Sun, and J. Zhao. Automatic Vehicle Tracking with Roadside LiDAR Data for the Connected-Vehicles System. *IEEE Intelligent Systems*, 2019. https://doi.org/10.1109/MIS.2019.2918115.

47. Lv, B., H. Xu, J. Wu, Y. Tian, Y. Zhang, Y. Zheng, C. Yuan, and S. Tian. LiDAR-Enhanced Connected Infrastructures Sensing and Broadcasting High-Resolution Traffic Information Serving Smart Cities. *IEEE Access*, Vol. 7, 2019, pp. 79895–79907. https://doi.org/10.1109/ACCESS.2019.2923421.

48. Sun, Y., H. Xu, J. Wu, J. Zheng, and K. M. Dietrich. 3-D Data Processing to Extract Vehicle Trajectories from Roadside LiDAR Data. *Transportation Research Record*, Vol. 2672, No. 45, 2018, pp. 14–22.

https://doi.org/10.1177/0361198118775839/ASSET/IMAGES/LARGE/10.1177_0361198118775839-FIG3.JPEG.

49. Zhao, J., H. Xu, H. Liu, J. Wu, Y. Zheng, and D. Wu. Detection and Tracking of Pedestrians and Vehicles Using Roadside LiDAR Sensors. *Transportation Research Part C: Emerging Technologies*, Vol. 100, 2019, pp. 68–87. https://doi.org/10.1016/J.TRC.2019.01.007.

50. Li, Y., Y. C. A. Tok, Z. Sun, S. G. Ritchie, and K. Allu. *Vehicle Point Cloud Reconstruction Framework for FHWA Axle-Based Classification Using Roadside LiDAR Sensor*. 2021.